Health Physics Pergamon Press 1961. Vol. 5, pp. 179–202. Printed in Northern Ireland

704625

REPOSITORY Joe - Forrestal
COLLECTION Markey Files
BOX No. 3 of 6
FOLDER Criticality Machine & Source Accidents

DOSIMETRIC INVESTIGATION OF THE YUGOSLAV RADIATION ACCIDENT*

G. S. HURST, R. H. RITCHIE, F. W. SANDERS, P. W. REINHARDT, J. A. AUXIER, E. B. WAGNER, A. D. CALLIHAN and K. Z. MORGAN
Health Physics Division, Oak Ridge National Laboratory, Oak Ridge, Tennessee†

(*Received* 3 *November* 1960)

Abstract—A complete investigation of the radiation doses received by individuals exposed to radiation in the Yugoslav accident on 15 October, 1958, has been completed, using modern techniques of dosimetry. The zero power reactor was operated at low power levels to determine the ratio of γ-ray to neutron dose at various locations near the reactor. These measurements were made with special counting methods, one of which measured the neutron dose in the presence of γ-rays, and the other measured the γ-dose in the presence of neutrons. The reactor was operated at a higher power level for a short time to determine (a) the neutron dose by means of threshold detectors and (b) the relationship between neutron dose and Na^{24} activation in man-shaped phantoms. A computational program gave theoretical results for the same three quantities, i.e. the neutron spectrum, the γ–neutron ratio, and Na^{24} activation. The results of theory and experiment are in good agreement.

Final results for the individual doses are shown in Table 7. In this table the charged particle dose refers to the first collision dose due to recoils from fast neutrons and includes the dose delivered by the nitrogen n–p reaction. The second dose column gives the maximum dose obtained for the hydrogen capture γ-radiation produced in the phantoms. The external gamma dose based on the measured γ–neutron ratio is shown in the third column, and the total doses are given in the last column. Of the seven persons investigated, the highest dose received (individual V) was 436 rads and the lowest dose was 207 rads. The doses previously estimated were reported in rem units, showing for individual V an estimated value of 210 rems for the neutron dose and 630 rems for the γ-dose, or a total exposure of 840 rems.

1. DESCRIPTION OF THE ACCIDENT

THE radiation accident[1] which occurred at the Boris Kidrič Institute on 15 October, 1958 resulted in heavy exposure of six young scientists to a mixture of neutrons and γ-radiation during the course of a subcritical experiment with a zero power reactor. The reactor[2] was constructed with natural uranium rods suspended in a large tank which could be filled to various depths with heavy water, and was primarily intended as a combined training and criticality research facility. Further details of the circumstances leading to the incident and of the reactor itself are described in the publications[1,2] from the Boris Kidrič Institute.

Following a brief period of hospitalization in Belgrade, the six patients were transferred to the Foundation Curie in Paris, and placed under the care of Dr. H. JAMMET. A summary of clinical observations, patient management, and dose estimates is described by JAMMET *et al.*[3] These dose estimates, from 1000 to 1200 rems for the highest exposure and from 300 to 500 rems for the lowest, placed five of the six individuals into a range of exposures which is considered to be above the lethal (LD-50) level. It is reported[4] that the hematological observations tended to confirm the physical dose estimates. Following these observations the

* Appendix E is by J. W. SMITH, United Kingdom Atomic Energy Authority, Harwell, England.

† Operated by Union Carbide Corporation for the U.S. Atomic Energy Commission.

1005280

highest exposed individual (V) was given fetal bone marrow on 11 November, and the four patients having the next highest exposures were given bone marrow from adult donors at various times between 11 November and 20 November. All of the patients except V recovered.

2. METHODS OF DOSIMETRY

The methods of dosimetry used to investigate the doses received by the individuals exposed in the Yugoslav accident were essentially those used in connection with the Oak Ridge Y-12 accident.[5,6] An outline of the general scheme is as follows. When fast neutrons enter the human body most of these are moderated to thermal energy and a small fraction of these are captured by a (n, γ) process in the Na^{23} in the body giving rise to Na^{24} which, by virtue of its emission of high-energy γ-rays with a radioactive half life of 14.8 hr, is easily detected. It has been shown (HURST *et al.*[6], Fig. 1) that the probability of neutron capture to make Na^{24} is not a strong function of the energy of the fast neutrons and that the probability of capture for neutrons in the fast region is higher than the probability of capture in the thermal region. Thus the uniform distribution of Na^{23} in the human body provides an excellent means of normalizing the neutron exposure of an individual. In particular, for a given neutron energy spectrum the fast neutron dose is proportional to the ratio Na^{24}/Na^{23} in the body or in the blood system. This method of normalization is quite important in the dosimetry of radiation accidents since no assumptions need be made about the exact location of an individual at the time of the energy release. The importance of this fact can be made clear by reference to the Y-12 accident[5] where it was shown, by calculating the neutron dose based on the known number of fissions and the stated location of the individual, that one of the surviving individuals would have received a dose several times the lethal value. Thus little credence can be placed in calculations requiring such assumptions.

More specifically, the determination of the neutron dose, D_n, and the γ-dose, D_γ, may be obtained from three quantities, $(D_n/a)_c$, $(D_\gamma/D_n)_c$, and a, which are related as follows:

$$D_n = (D_n/a)_c \times a$$
$$D_\gamma = (D_\gamma/D_n)_c \times D_n$$

where the quantity $(D_n/a)_c$ is the neutron dose per unit sodium activation which is characteristic of the type of source and the exposure conditions, a is the measured amount of sodium activation within the individual, and $(D_\gamma/D_n)_c$ is the ratio of γ-dose to neutron dose which is characteristic of a given source and set of exposure conditions. In both the Y-12 and Vinča accident investigations the quantity $(D_n/a)_c$ was determined by two methods, experiment and theory. The experimental method at Vinča consisted of measuring the neutron dose (with a Radsan fast neutron dosimeter[7]) required to produce a given amount of activation in a plastic man-shaped phantom filled with an aqueous solution of NaCl. The ratio $(D_\gamma/D_n)_c$ was determined with two types of γ-dosimeters,[8,9] and the Radsan neutron dosimeter. The quantity a was based on the Na^{24} analysis reported by JAMMET *et al.*[3] As a supplement and check on the experimental procedure, the quantities $(D_n/a)_c$ and $(D_\gamma/D_n)_c$ were calculated for the zero power reactor. In addition to the quantities D_γ and D_n, it is desirable to determine the neutron spectrum $N(E)$. This was done by calculation and by experiment using the series of threshold detectors[10,11] developed for this purpose.

3. EXPERIMENTAL INVESTIGATIONS

To accomplish the measurements indicated above, the zero power reactor (Fig. 1) was operated in two different ranges of power level which for convenience will be referred to as "low" power and "high" power. Fig. 2(a) shows the general location of the dosimetry equipment for the low- and high-power runs. The LPS stations show locations where most of the dose measurements were made, the V.T. and H.T. represent, respectively, locations where vertical and horizontal traverses were made with Au and S detectors during the high-power runs. Figs. 2(b) and 2(c) show the location of the phantoms for high-power runs at 1 kW and 5 kW, respectively. To facilitate intercomparison of data obtained from the two types

1005281

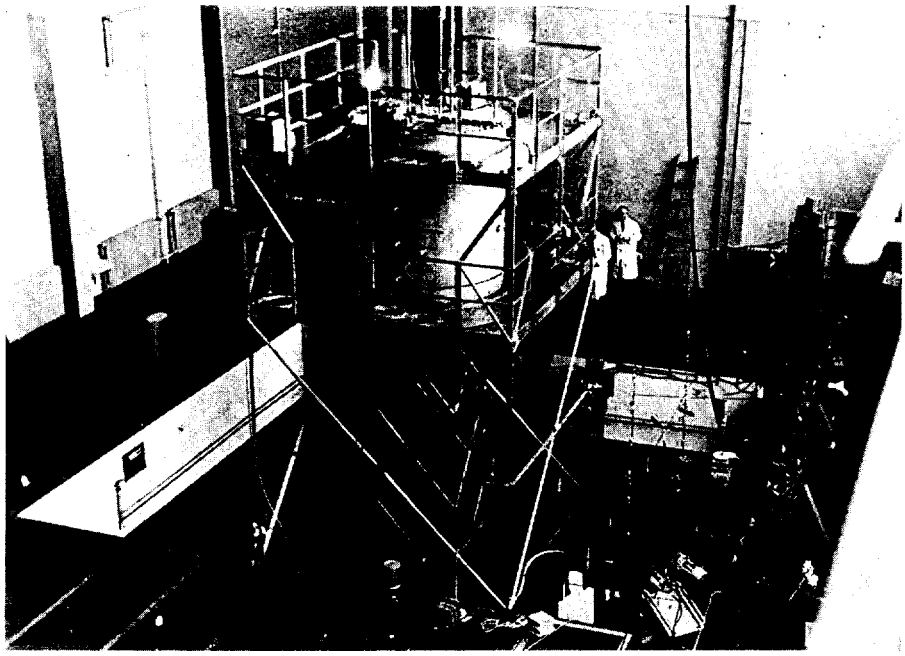

FIG. 1. Zero power reactor.

1005282

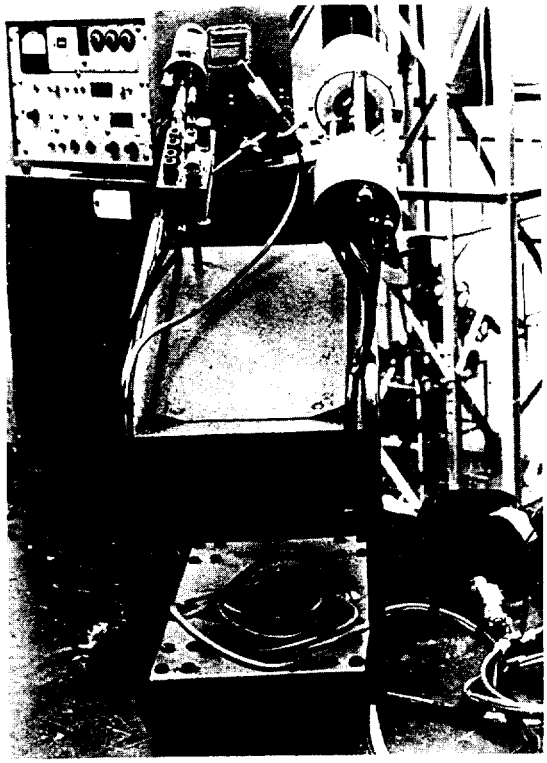

FIG. 3. Mounting arrangement for the low-level dosimeters.

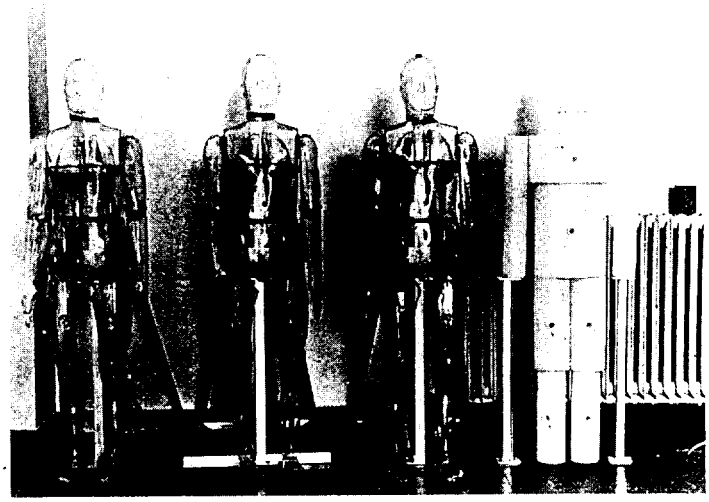

FIG. 4. The four plastic phantoms—Calvin, Remab, Tyrone and Bomab.

1005283

PRIVILEGED

Y

The following was taken from a letter of November 27, 1958 from Dr. D. W. van Becqum, Rejswijk, to Dr. Otto Voss, Biology Division, Oak Ridge:

"This material should be handled as confidential until is is released by the French physicians.

"Of the six people who were in the accident in Yugoslavia five were male and one female. They got neutron and gamma radiation by working with a sub-critical device that suddenly became critical by accident. (Remarks by Dr. A. Hollaender: It seems to be a very similar accident to the one which took place at Los Alamos several years ago and had very serious implications).

"The accident happened on October 14, and on the 16th all patients and three Yugoslavian physicians went to Paris to the Curie Hospital. Absolute dosage was not known but thought high. On the basis of the blood picture, it was deduced that one man got sub-lethal dose, four got lethal doses and one person got considerably higher than lethal dose. In 3-4 weeks it was recognized that it was urgently necessary to use bone marrow transplantation. The patient who had super-lethal dose received about one billion embryonic spleen cells. These were given by Dr. Matte and Dr. DuPlan. No sign of regeneration was apparent in this case and after two days some abdominal complications occurred. It was thought much too dangerous to operate on this patient to determine the source of the abdominal complication. Ten to fifteen billion adult bone marrow cells were injected in this over-exposed patient. Uremia was observed. An artificial kidney was used. Following this, massive bleeding occurred. This patient died and an autopsy was performed which showed some complication in the stomach and in the ilium and the bone marrow in the autopsy showed obvious signs of regeneration. The man mentioned previously who had received a considerably sublethal dose did not need a bone marrow transplant and is improving rapidly. The other three males and one female all were given 10-15 billion adult bone marrow cells between November 10-14. Each transplant came from one donor. The reaction in the blood picture was enormous after only two days and an obvious increase of all blood elements was found. (This is Dr. van Becqum's statement: "I don't know about the lymphocytes').

"In the first transplant case (of the four "lethal" cases--CLD) the donor cells can be recognized by blood typing (so we have a French-Yugoslavia chimera). To obtain this amount of bone marrow from one donor at least 18 punctures were necessary: sternum, ribs, iliec crests and spinal column were used. This was done under complete anesthesia. The blood groups were determined very well so that donor cells could be recognized in the recipient. The girl got female bone marrow because of Bichwald--Simmonn effect. Cohen, van Tutten were in Paris yesterday and saw everything. The people cooperated very well.

"I was very pleasantly surprised at how well Dr. Matte proceeded with all of the different stops. Of course, we are all anxious to see if these people will get secondary reactions or other complications, and we will be watching them very closely to see what happens. Dr. van Tutten is staying on in Paris to be present if any complications should come up."

1005284

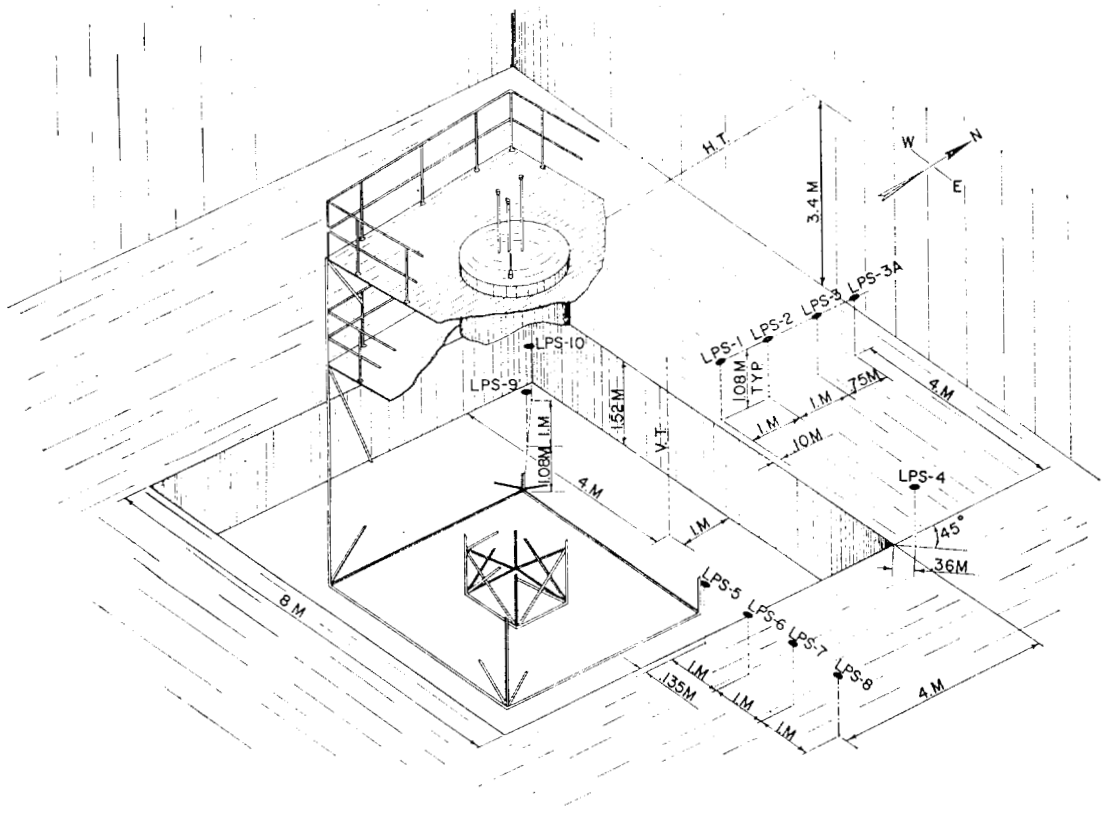

FIG. 2(a). Dosimetry station locations in reactor room.

of operating conditions, a sulfur pellet was placed at a convenient location on the side of the reactor tank before each run.

3.1. *Low-power experiment*

The ratio of γ-dose to fast neutron dose was measured at some of the positions shown in Fig. 2(a), using the equipment mentioned above (mounted as shown in Fig. 3) and with the reactor operating at a power level of approximately 5 W.* The results of the directly measured ratio, D_γ/D_n, are shown in Table 1 which gives also the neutron dose, as measured with Radsan, per unit monitor flux density (i.e. sulfur neutrons/cm^2). The final D_γ/D_n values for the various positions are based on the

Table 1. *Experimental values for D_γ/D_n at various positions*

Position (LPS no.)	Neutron dose per unit monitor (rad/n cm^{-2})	D_γ/D_n
1	1.13×10^{-6}	3.5
2	0.90×10^{-6}	3.6
3	0.75×10^{-6}	3.6
3a	0.66×10^{-6}	3.9
4	0.64×10^{-6}	3.8
8	0.54×10^{-6}	3.5
9	0.86×10^{-6}	4.0
10	0.72×10^{-6}	4.2

* Private communication with D. Popović indicated that the power calibration in the initial run yielded a figure approximately 0.56 times the value quoted here. This correction factor applies to all power levels quoted in the remainder of this report.

1005285

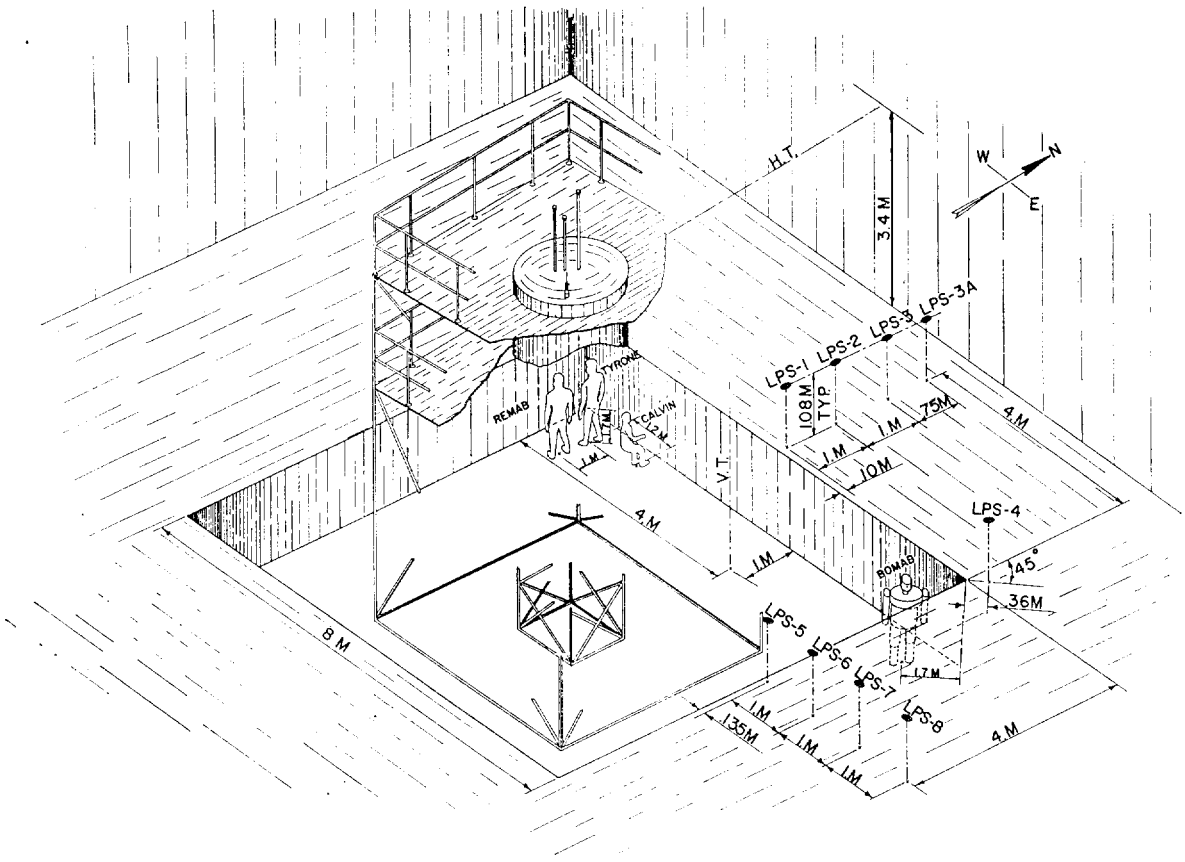

FIG. 2(b). Dosimetry stations and phantom locations in reactor room.

counting method of γ-ray dosimetry described by WAGNER and HURST[8]. The carbon–CO_2 chamber[9] used in this experiment gave results which were 1.3 times the dose values obtained with the counting method, but later studies with the carbon–CO_2 chamber at ORNL showed that it has an appreciable response to thermal neutrons.

3.2. *High-power experiment*

With the reactor operating first at 1 kW, then at 5 kW, two types of measurements were made, neutron spectrum measurements and Na^{24} activation in man-shaped phantoms. The spectral measurements were made with threshold detectors[10,11] located at various positions (stations). The results obtained for Stations 1, 9 and 10 are shown in Table 2, where comparison is made with the spectral data obtained for the Y-12 excursion with the same type of detectors.

Table 2. Experimental information on neutron spectrum (ratio of flux above threshold of various detectors to total fast flux)

Threshold detector	Boris Kidrič (ZPR) threshold energy			Y-12 excursion
	Sta. 1	Sta. 9	Sta. 10	
Pu	1.00	1.00	1.00	1.00
Np	0.36	0.35	0.35	0.89
U	0.20	0.18	0.19	0.54
S	0.094	0.088	0.090	0.25
Au	3.91	3.63	3.87	0.45

100528b

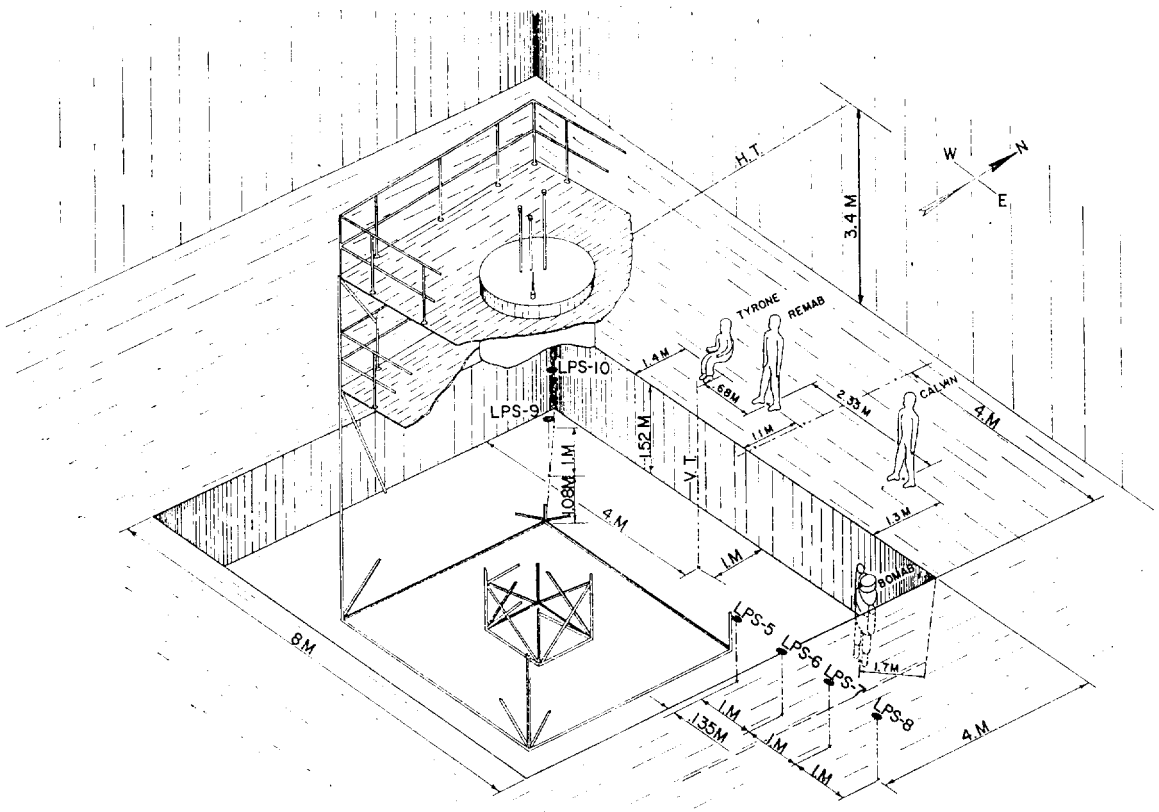

FIG. 2(c). Dosimetry stations and phantom locations in reactor room.

Sodium activation data were obtained by locating phantoms (Fig. 4) at the positions shown in Fig. 2(a). During the 1-kW run the phantoms were located as shown in Fig. 2(b), and during the 5-kW run they were as shown in Fig. 2(c). The phantoms were filled with an aqueous solution of NaCl at a concentration of 15.7 mg Na^{23} per gram of solution. After irradiation the sodium activation, a (in units of μc Na^{24}/mg Na^{23}) was determined according to the technique described in ORNL-2748A.[12] From the data obtained during the low-power experiment, Table 1, and by normalizing the relative exposure in some cases by means of the activation of sulfur pellets placed on the phantoms, the neutron dose received by the phantoms was obtained. The results of $(D_n/a)_c$ are shown in Table 3, where each entry corresponds to the weighted average value of a for all the compartments of the phantom. Further experimental data are given in Appendices A, B, C and D. In particular, Appendix B justifies

Table 3. Neutron dose per unit sodium activation for man-shaped phantoms exposed at the zero power reactor

Phantom	$(D_n/a)_c$ (rad μc^{-1} mg Na)	
	1-kW run	5-kW run
Tyrone	9.12×10^4	7.73×10^4
Remab	8.57×10^4	8.13×10^4
Calvin	9.12×10^4	7.27×10^4
Grand average = 8.65×10^4		

1005287

the particular way in which the phantoms were used in this experiment.

4. THEORETICAL INVESTIGATIONS

In this section a description will be given of the methods used in calculating neutron and γ-leakage from the Boris Kidrič zero power reactor in the critical and near-critical state. The methods used are entirely theoretical in the sense that they rely not at all upon measurements which were made at Vinča. Multiple scattering of leakage radiation in walls and structure of the reactor building are neglected and only direct leakage of neutrons and γ-rays from the assembly is considered. As shown below by comparison with experimental data, this approximation is surprisingly good, although the agreement may be fortuitous in some particulars.

The quantities presented are: (1) $N_n(E)$, the neutron leakage spectrum; (2) $D_n(E)$, the neutron first collision dose leakage spectrum; (3) D_n/a, the ratio of the total first collision dose received by an idealized phantom to the Na^{24} activation generated in the phantom by the leakage spectrum incident upon it; and (4) D_γ, the γ-ray first collision dose leaking from the reactor due to the fission process and due to various neutron capture processes occurring in and around the reactor.

The method of computing neutron leakage which has been used in this work is the multigroup-diffusion approach. An existing criticality code written for the IBM-704 which automatically computes neutron leakage in several energy ranges has been employed. The computing time for this code is quite modest for most systems. γ-Ray leakage is treated by special IBM-704 codes. The method uses known γ-ray cross-sections and build-up factors to calculate attenuation kernels for the particular medium under consideration. The radiation field at various points inside or outside the assembly is then computed by summing over source points in the assembly, using best estimates available for the γ-ray spectra of the various sources. The spatial distribution of fissions in the assembly is obtained from the neutron leakage runs and is used in the γ-leakage calculation.

4.1. *Neutron leakage spectrum*

The method which was employed to calculate the neutron leakage spectrum from the Vinča reactor is based primarily upon the use of a multigroup, multiregion reactor analysis code[13] for the IBM-704. The basic equation solved by the code is the multigroup-diffusion approximation to the Boltzmann transport equation. The program approximates the differential equation by a difference equation and allows as many as 250 space points and forty-four energy groups in the solution of the resulting equations.

Since the Boris Kidrič reactor uses a lattice spacing which is quite small (12 cm) compared with the outside dimensions of the reactor, it should be a good approximation to consider an equivalent homogenized reactor.[14] The unit lattice cell was taken to be cylindrical with a fuel rod at its center and containing the same quantity of D_2O as the real unit lattice cell. A preliminary multigroup calculation of the distribution of flux inside this cell was made, using the boundary condition of zero total current at the outer boundary of the equivalent cylindrical cell. Homogenized multigroup cross-sections were computed using the calculated flux distribution as a weighting function. A multigroup calculation of the escape spectrum for the entire reactor was then made with these cross-sections, assuming that a 1-cm layer of aluminum surrounded the volume. Fig. 5 shows a plot of the multiplication factor, k, of the assembly as a function of height. On the same graph is shown the total neutron leakage per fission neutron in the core as a function of height. One sees that this calculation predicts a critical height of approximately 185 cm, compared with the experimental value[2] of 177.6 cm. It is felt that the agreement is sufficiently accurate for our purposes, since the neutron leakage varies by only approximately 4 per cent over the range of heights. It is possible that back-scattering of neutrons from the tank supporting members and from the walls of the room might well account for the difference between experimental and calculated values of the critical height. These results also show that there is negligible difference between neutron leakage per fission neutron in the critical state and in the delayed supercritical state which occurred at the time of the

1005288

accident. Estimates of the $k_{ex} = k - 1$ appropriate to the excursion[15] show that $k_{ex} \simeq 10^{-3}$. According to Fig. 5 the neutron leakage per core neutron at this value of k_{ex} is only approximately 2 per cent different from that in the steady state.* Hence, this difference will be neglected in the remainder of this calculation.

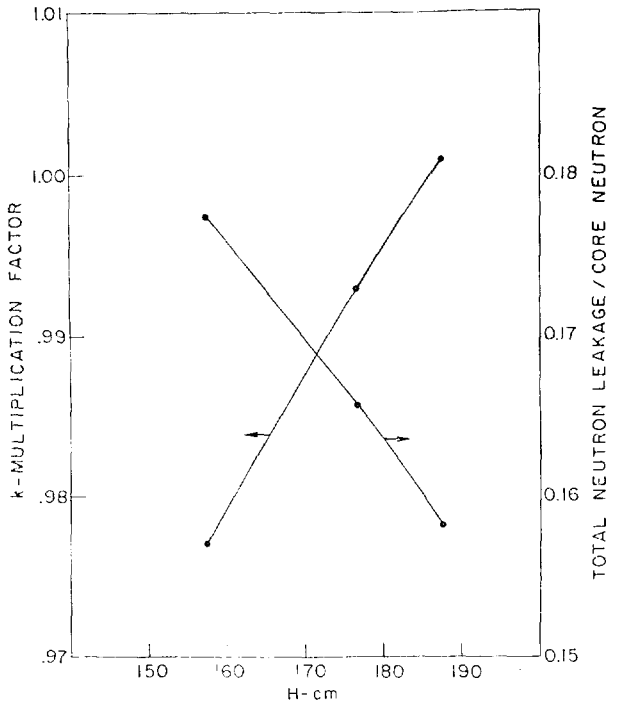

FIG. 5. Multiplication factor and total neutron leakage as a function of height.

Fig. 6 shows the neutron leakage spectrum calculated for the reactor at the critical level.† The quantity plotted in the ordinate is $EN(E)$, and the abscissa gives both the energy E and the lethargy $u = \ln[10/E(\text{MeV})]$. The spectrum is conveniently represented in this way since the number of neutrons escaping between any two energies is just proportional to the area under the portion of the curve between these energies. The total fast leakage in this spectrum is 0.234 neutron per fission while the leakage in the thermal group is 0.157 neutron per fission.

The first collision dose spectrum for neutrons is shown in Fig. 7. The factor $D_0(E)$ is the first collision dose per unit neutron flux.[17] $\int_0^\infty D_0(E)\, N(E)\, dE$ is found to be 4.37×10^{-11} rad cm^2/core neutron.

To make possible a comparison with experimental measurements of D_n, a calculation of $(D_n)_R = \int_0^\infty D_{\text{Radsan}}(E)\, N(E)\, dE$ was carried out. $D_{\text{Radsan}}(E)$ is the dose measured by the Radsan fast neutron dosimeter at energy E and is less than $D_0(E)$ at low energies due to bias losses. Values of $D_{\text{Radsan}}(E)$ were inferred from the work of WAGNER and HURST[18]. The result of this calculation was $(D_n)_R = 3.12 \times 10^{-11}$ rad cm^2 per core neutron.

* A change in the leakage per fission neutron with k would not, by itself, affect the result of this dosimetry study. A radical change in the neutron spectrum, on the other hand, would produce a change in the ratio of D_n/a and would mean that experimental work with a steady operating reactor would not be comparable with conditions obtaining during the accident. However, comparison of the calculations at different values of k indicates negligible change in the spectrum between the two reactor states.

† This spectrum is somewhat different in the low energy range from a preliminary result given elsewhere.[16] Improved values of the homogenized multigroup cross-sections were used in the present calculations.

1005289

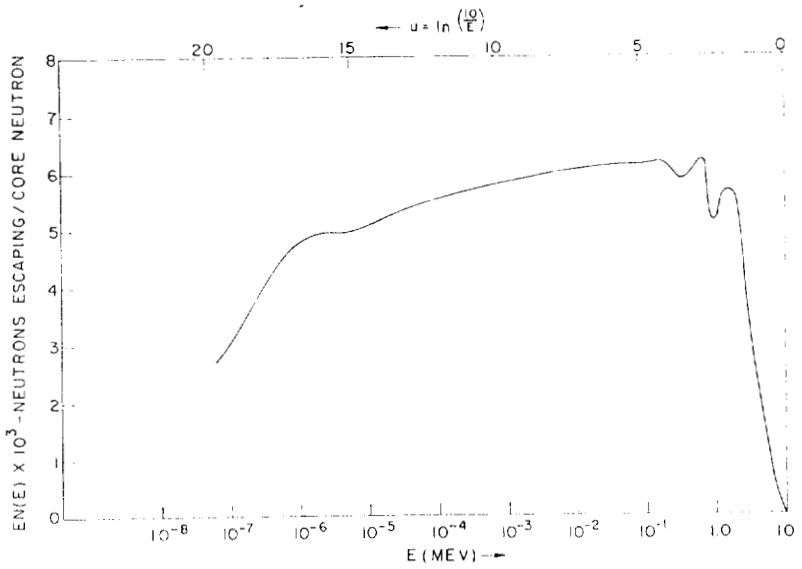

FIG. 6. Escape neutron spectrum.

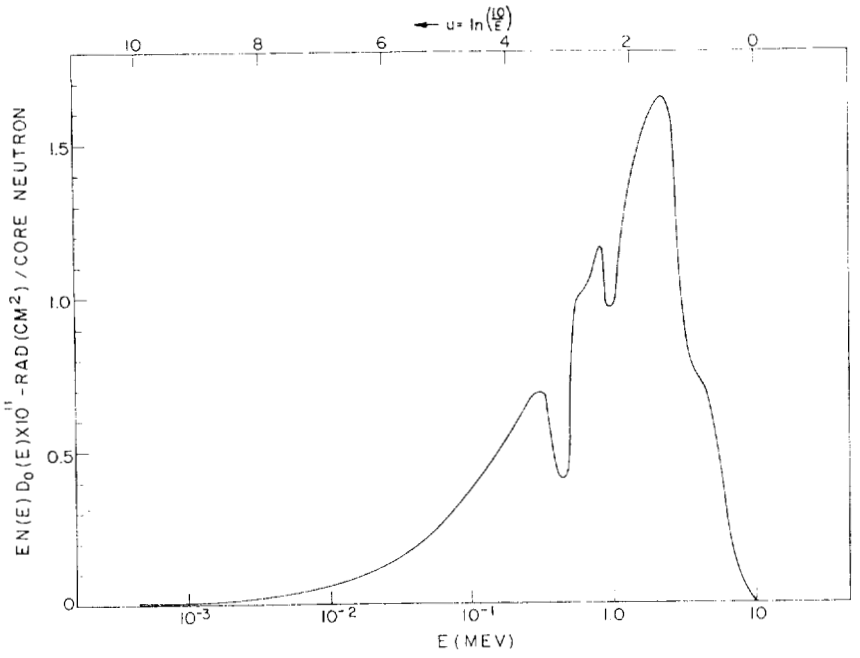

FIG. 7. Neutron dose spectrum from reactor.

1005290

In order to calculate a, the Na^{24} activation induced in a man exposed to the calculated spectrum, use was made of approximate results for $\xi(E)$,[6] the capture probability at thermal energy per unit flux of neutrons incident normal to the axis of a circular cylinder of 15 cm radius. Using the function $\xi(E)$, the quantity $(D_n)_R/a$ was calculated from

$$\frac{(D_n)_R}{a} = 1.12 \times 10^{11} \frac{\int_0^\infty D_0(E)\ N(E)\ dE}{\int_0^\infty \xi(E)\ N(E)\ dE} \times \frac{\text{rad}}{\mu\text{c g of Na}^{23}}$$

$$= 7.2 \times 10^4 \text{ rads}/\mu\text{c (mg Na)}^{-1}$$

and compares favorably with the average value of 8.65×10^4 rads/μc (mg Na)$^{-1}$ obtained with the phantoms (see Table 3).

The multigroup computation of the leakage spectrum takes into account the neutron distribution in only one spatial dimension and introduces an artificial absorption to account for leakage transverse to the direction in which computation proceeds. Within the framework of multigroup diffusion theory, one may take into account the dependence of the leakage flux with direction with respect to the reactor axis.[16] This has been done in the comparisons given in Table 4.

Other comparisons can be made between the experimental determination and the calculation of the leakage spectrum by use of the activation of the threshold detectors which were exposed during the work at Vinča. Table 5 shows a comparison of various ratios calculated from the spectrum given above with experimental determinations of these ratios. The experimental values represent station averages. The quantity $\phi_{>E_T}$ represents the neutron flux lying above the effective energy threshold of E_T MeV in the case of various detectors. The quantity $4\pi R^2(D_n)_R/F$ was obtained from the experimental data by employing the Radsan-measured neutron dose rate together with the fission rate, F, occurring inside the assembly. The fission rate was obtained from a power calibration performed by the Yugoslav experimenters.[19] For the purpose of comparison with experiment, the theoretical values have been corrected, approximately, for the non-$1/R^2$ variation of the dose at points in the neighborhood of the reactor.

Table 4. Summary of $4\pi R^2 \times$ dose due to various sources

γ-Source	$D\gamma \times 10^{10}$(r cm^2/fission)		
	Station 1	Station 9	Station 10
Prompt fission	1.77	1.46	1.63
$U^{238}(n,\gamma)U^{239}$ capture	0.77	0.63	0.69
Moderator capture	0.05	0.05	0.05
Tank 2nd structure capture	~0.30	~0.30	~0.30
Fission products during experiment	1.12	0.92	1.03
Total dose during experiment	4.01	3.36	3.70
Fission products during accident	0.39	0.32	0.36
Total dose during accident	3.28	2.76	3.03
	Dose ratios (r/rad)		
$D\gamma/(D_n)_R$ calculated for experiment	3.52	3.00	3.40
$D\gamma/(D_n)_R$ measured for experiment	3.5	4.0	4.2
$D\gamma/(D_n)_R$ calculated for accident	2.88	2.46	2.78
	$(D_n)_{\text{Radsan}} \times 10^{10}$ (rad cm^2/fission)		
Leakage neutrons	1.14	1.12	1.09

4.2. *γ-Dose leakage*

There are many sources of γ-radiation in and around the reactor which should be considered. It will be seen that reasonably good estimates of the dose from most of them may be made. Although the uncertainties in these estimates are likely to be as much as 20 per cent, it is clearly worthwhile to make such calculations in order to understand better the physics of the accident. Each of the sources of γ-radiation

1005291

Table 5. Comparison of calculated and experimental dose and flux ratios

Ratios	Experiment	Theory
$\frac{(D_n)_R}{\phi_{>2.5}} \times 10^8 \left(\frac{\text{rad cm}^2}{\text{neutron}}\right)$	1.6	1.55
$\frac{4\pi R^2 (D_n)_R}{F} \times 10^9 \left(\frac{\text{rad cm}^2}{\text{fission}}\right)$	0.90	0.77
$\frac{\phi_{>1.5}}{\phi_{>2.5}}$	2.1	2.32
$\frac{\phi_{>0.7}}{\phi_{>2.5}}$	3.8	3.84
$\frac{\phi_{>0.01}}{\phi_{>2.5}}$	11.3	15.6
Gold foil—cadmium ratio	3.5-6.5	4.9

have been considered in turn with a detailed description presented in the Appendices.

4.2.1. *Prompt γ-rays from the fission process and capture γ-rays from the* U^{238} (n, γ) U^{239} *process.* The distribution in energy of prompt fission γ-rays is taken from the work of MAIENSCHEIN *et al.*[20] The energy distribution of γ-rays from the $U^{238}(n, \gamma)U^{239}$ process is taken from the work of BARTHOLOMEW and HIGGS[21]. In order to calculate the escape of these photons from the reactor, one must consider both attenuation in the uranium rods and in the D_2O. Some simplifying assumptions were made in order that leakage from this very inhomogeneous system could be estimated in a reasonably short computing time. For the purpose of calculating leakage the distribution of fissions in a given fuel rod was assumed to be flat in the radial direction and to depend only on position along the length of the rod. The attenuation of γ-rays in the fuel rod in which they originate is accounted for, but their attenuation in other fuel rods is neglected. This approximation should result in little error since the rods are small in diameter compared with the lattice pitch. The computation proceeds by a numerical integration of the product of the source strength and leakage probability for each element in the source. The photon source distribution is obtained from the neutron criticality calculation described above. The attenuation of photons in traveling from a given source point to a field point outside of the reactor is calculated using tabulated photon attenuation coefficients[22] and infinite medium build-up factors for the part of the path lying inside of the reactor. The error involved in using these build-up factors should be small in the cases which we shall consider. A more detailed description of the computational procedure is given in Appendix A.

The leakage probability is a function of the distance from the reactor and the angle which the vector to the field point makes with the axis of the reactor. The results for some of the stations are given in Table 4 and are expressed as $4\pi R^2$ (dose/fission) at the respective stations, where R is the distance from the center of the reactor to the various stations.

4.2.2. *γ-Rays from fission products.* The estimate of this contribution is uncertain owing to the fact that it depends to some extent upon the movement of the exposed persons after the reactor scram. In view of this uncertainty this fraction of the total dose received was approximated. The attenuation kernel of fission product γ-rays in the lattice was taken to be the same as that of prompt fission γ-rays and further it was assumed that the first can be estimated by scaling the second according to the relative energy released in the two processes. Details of this estimate are given in Appendix B, and Table 4 shows the results for Stations 1, 9, and 10 for two different cases: (1) at 15 min after the beginning of a steady power level run (in this case the dose values should be interpreted as r/sec per fission/sec); and (2) 4 min after the beginning of an excursion with a doubling time of 10 sec. The dose values refer to the total fission product γ-dose received during the interval per fission occurring.

4.2.3. *γ-Rays from capture in moderator and fuel cladding.* The thermal utilization, f, for the reactor was calculated by multigroup methods to be 0.9865 for an assumed concentration of 0.16 per cent H_2O in the moderator. Assuming that all of these captures occur in hydrogen nuclei and noting that c, the moderator capture

1005292

probability per fission in the critical state, is equal to $(1 - f)/b$, where b is the ratio of fission to total capture probability in the fuel, it follows that

$$c = \frac{1 - f}{b} = \frac{0.0135}{0.543}$$

$$= 0.0349 \text{ moderator captures/fission}$$

A calculation of the leakage of hydrogen capture γ-rays from the homogenized reactor gave $\sim 0.5 \times 10^{-10}$ rad cm^2/fission for the three stations considered (Table 4). The same multigroup calculation showed the capture probability in the aluminum cladding around the fuel rods to be 0.00642 captures per total capture. The dose due to this source would be expected to be even smaller than that due to captures in the moderator, especially since attenuation of these photons in the fuel rod should make the effective source strength even smaller; thus it has been neglected in Table 4.

4.2.4. *γ-Rays from capture in tank walls and supporting structure.* This source of photons is difficult to estimate accurately because of the very complicated configuration of materials, chiefly aluminum, in the immediate neighborhood of the assembly. A rough estimate, assuming that the structural aluminum may be considered equivalent to a 2-cm layer enveloping the whole reactor, gives 3×10^{-10} r cm^2/fission in the region around the reactor.

4.2.5. *γ-Rays from capture in walls and floor of reactor room.* This contribution is very difficult to estimate with any accuracy and hence was not considered.

4.3. *Discussion*

The chief uncertainties in the estimates given above are: (1) use of infinite medium build-up factors rather than those appropriate to a finite medium; (2) neglect of photon attenuation in rods other than that on which a given photon originates; and (3) neglect of photons from neutron capture in reactor room materials and in air of room. The net uncertainty in the calculation is estimated to be $\sim \pm 20$ per cent. The ratio of the γ-doses during the accident to corresponding doses during the experiment, f, should be more accurate than this and consequently this ratio will be used to correct the experimental data.

Table 4 also shows the neutron dose, $(D_n)_{\text{Radsan}}$ at the three stations considered. These values were estimated by taking into account the angular distribution of radiation leaving the reactor and correcting for the finite size of the reactor by using a radiation center displaced 0.8 m toward a given station from the center of the reactor. Also shown in this table are the values of D_γ/D_n inferred from the above estimates and a comparison of these values with those measured during the experiment.

5. ASSIGNMENT OF INDIVIDUAL DOSES

In previous evaluations of dose received by man, the usual procedure has been to evaluate the first collision dose for both neutrons and γ-radiation. That procedure was followed because of the difficulty of specifying a dose within the body which would have the desired radiobiological significance. This procedure has been justified on the basis that if the first collision doses are determined along with certain additional exposure conditions (i.e. angular and spectral distribution of the incoming radiations) more elaborate correlations of medical effects and exposure doses may be carried out at future times when more detailed biological mechanisms are understood or are being tested. In the case of the Y-12 exposures, the first collision dose for γ-radiation and fast neutrons and the neutron and γ-ray energy distributions are given. In the present case, however, it appears advisable to comment on the γ-radiation which is produced by the capture of low-energy neutrons by the $H(n, \gamma)$ reaction. Based on the neutron spectrum (Section 4) and the calculations by SNYDER,[23] it may be seen that the additional γ-dose near the surface of a 30-cm slab makes an appreciable contribution to the total dose at that point.

We separate the neutron exposure into two dose components, namely (1) the first collision charged particle dose made up of thermal neutron interactions of the type $N^{14}(n, p)C^{14}$ and recoil atoms (H, C, N, O) from fast neutron interactions; and (2) the autointegral γ-dose at the surface of the slab due to the $H(n, \gamma)D$ process.

1005293

Data are not presently available which enable one to calculate the H(n, γ)D autointegral dose for a realistic model of a man bombarded with neutrons. However, there are data[23] on the autointegral dose in a slab due to normal irradiation by neutron beams of various energies. These data are conservative in the present connection, i.e. the doses obtained using these values will surely represent overestimates of the autointegral doses to a man and may be too large by a factor of 2.

energy lost under the bias of the neutron dosimeter, as derived in Section 4.

The first collision γ-doses (external doses) for the individuals may be expressed as

$$(D_\gamma)_{\mathrm{G,D,B}} = \frac{3.6}{1.4} \times 0.82 \text{ (charged particle dose)}_I$$

$$(D_\gamma)_{\mathrm{H,V,M}} = \frac{4.1}{1.4} \times 0.82 \text{ (charged particle dose)}_I$$

where we have used the results of Table 1 for the quantities D_γ/D_n most appropriate to the

Table 6. Individual sodium activation and related data

Individual	Total Na^{24}(μc)	Wt. (kg)	Na^{24} (μc/mg Na)	$(W_I/W_p)^{1/3}$
H	53	65	5.44×10^{-4}	1.00
V	82	80	6.83×10^{-4}	1.08
G	76	70	7.24×10^{-4}	1.03
M	75	72	6.94×10^{-4}	1.04
D	63	52	8.07×10^{-4}	0.93
B	45	90	3.33×10^{-4}	1.12
(Phantom)		65		

The surface autointegral doses per unit neutron flux in the slab case were used to calculate the dose for the whole neutron spectrum, shown in Fig. 6. The result was found to be

$$[\mathrm{H}(n, \gamma)\mathrm{D} \text{ autointegral dose}]_I = 1.50(\text{charged particle dose})_I$$

It may be seen that

$$(\text{charged particle dose})_I = (\mu\text{c/mg Na})_I (W_I/W_p)^{1/3} \times \left(\frac{\text{charged particle dose to phantom}}{\mu\text{c/mg Na in phantom}}\right)$$

where I refers to the individual case and $(W_I/W_p)^{1/3}$ is a correction factor based on the weight W. From the experimental data obtained on the Na^{24} activation in the phantoms, Section 3, it may be seen that

$$\left(\frac{\text{charged particle dose to phantom}}{\mu\text{c/mg Na in phantom}}\right) = 1.40 \times 8.65 \times 10^4 \text{ rads}/\mu\text{c mg}^{-1}$$

where the factor 1.40 is a correction for the

individuals, and the factor 0.82 corrects the D_γ/D_n ratios as measured in the constant power reactor experiment to the values appropriate to the intensity–time relationship for the accident.

Table 6 shows the individual sodium activation as reported by JAMMET *et al.*[3], the weights of the individuals, and the magnitude of the factor $(W_I/W_p)^{1/3}$. The individual doses as determined by the equations above are shown in Table 7.

The main uncertainty in the dose values given in Table 7 is associated with the H(N, γ)D dose component. As already stated, this value may

Table 7. Individual doses (all values are in rad *units)*

Individual	Charged particle dose	H(n, γ)D γ-dose	External γ-dose	Total
H	66	99	158	323
V	89	133	214	436
G	90	135	189	414
M	87	130	209	426
D	91	136	192	419
B	45	67	95	207

1005294

be too high by a factor of about 2; however, even in this case, the total doses would be decreased only by about 15 per cent. The uncertainties associated with the other dose components are smaller; the standard deviations for the charged particle doses and for the external γ-doses are estimated to be $\pm$ 12 per cent and $\pm$ 14 per cent, respectively.

Work is now in progress on the study of Na^{24} activation in phantoms of various shapes and sizes and with neutrons of various energies. The question of biological elimination of Na^{24} is being investigated with living animals exposed at various dose levels. When these studies have been completed, it may be desirable to re-evaluate the individual doses received from the various radiation accidents, including the Y-12 (Oak Ridge) accident and the Yugoslavia accident.

APPENDIX A

γ-Dose Leakage Computations

A.1. *Computation of the leakage of γ-rays originating in fuel rods*

The computation proceeds by a numerical evaluation of the following integral:

$$D_\gamma(\mathbf{R}) = \int d\mathbf{r} S(\mathbf{r}) \frac{d_\gamma(|\mathbf{p}|,\vartheta)}{4\pi(|\mathbf{R} - \mathbf{r}|)^2}$$

where $\mathbf{R}$ is a vector from the center of the reactor to the field point where the leakage dose is desired, $\mathbf{r}$ is a vector from the reactor center to the volume element $d\mathbf{r}$ where the γ-source strength is $S(\mathbf{r})$, $\mathbf{p}$ is the part of the vector $\mathbf{R} - \mathbf{r}$ which lies inside the reactor volume, and ϑ is the angle between $\mathbf{R}$ and the cylinder axis. The source distribution function $S(\mathbf{r})$ is obtained from the neutron leakage calculation described above and is equal to the number of photons per fission times the normalized fission probability in the homogenized reactor.

The dose attenuation kernel $d_\gamma(\mathbf{r})$ is calculated by summing over the distribution of energies present in the particular source after weighting each energy component by an attenuation factor which is calculated using known absorption coefficients and build-up factors and a self-absorption factor to account for fuel rod attenuation. More specifically,

$$d_\gamma(r,\vartheta) = \int dE\, n_\gamma(E)\, \mathscr{D}_0(E)\, B[E, r\mu(E)] \times e^{-r\mu(E)}\, \mathscr{S}(E, \mu_r(E)a, \vartheta)$$

where r is the distance from an isotropic point source in an infinite D_2O medium, $\mathscr{D}_0(E)$ is the first collision dose in rads/photon $\times$ cm^{-2} delivered by photons of energy E, $\mu(E)$ is the mass absorption coefficient of the medium for photons of that energy, and $B[(E), r\mu(E)]$ is the build-up factor for photons in the medium. We have chosen to use infinite medium build-up factors even though the systems are bounded.[24] The error incurred in making this approximation should be approximately 10 per cent.

The self-absorption factor $\mathscr{S}(E, \mu_r(E)a_0, \vartheta)$ is calculated by carrying out an integral over the cross-section of the rod at radius a_0, using attenuation coefficients, $\mu_r(E)$, appropriate to natural uranium at the energy E, and taking into account the angle ϑ which the direction of observation makes with the axis of the rod. Build-up factors for the part of the photon path lying inside the rod were taken to be appropriate to the same distance, measured in g/cm^2, in the D_2O medium, as suggested by GOLDSTEIN and WILKINS[25]. As mentioned in Section 4.2.1, rod attenuation of photons not originating in a particular rod is neglected, since the rod radius is small in comparison with the lattice pitch.

Fig. 8 shows a graph of the attenuation kernel for the prompt fission γ-spectrum for the case of no rod absorption and for a natural uranium rod 1 in. in diameter viewed at various angles with respect to the rod axis. Note that the curve labeled $\vartheta = 14.5°$ is probably too small in magnitude since the simple ray path length approach used here will surely break down at grazing angles relative to the rod axis. A "short circuiting" effect will become important, i.e. photons emerging from the rod in directions nearly perpendicular to the axis may make collisions on D_2O molecules which will deflect them into directions nearly parallel with the rod axis. These photons may contribute in larger quantity than those taking longer paths through the rod. However, small values of ϑ are not required for the calculation of doses to any of the stations measured in the experiment.

Table 8 shows values of $4\pi R^2 D_\gamma$ vs. R for three

1005295

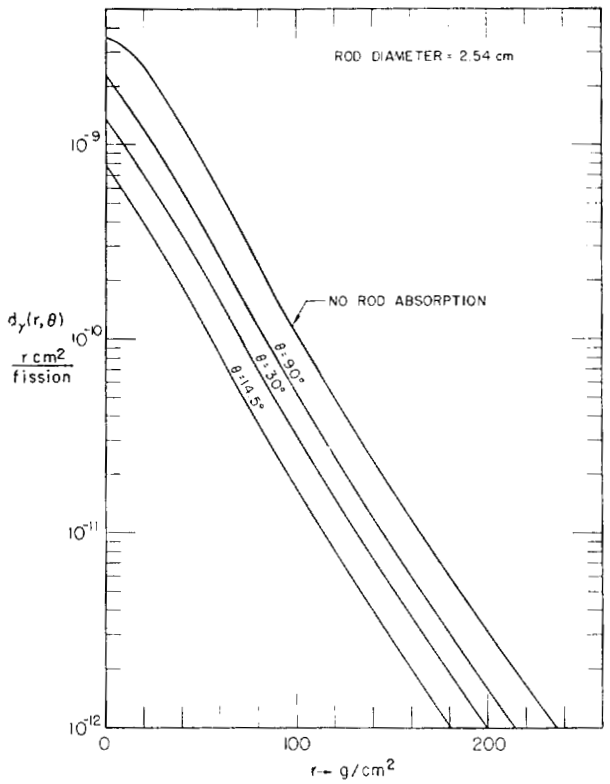

FIG. 8. Attenuation kernel for prompt fission γ-ray spectrum.

Table 8. Dose due to prompt fission γ-rays as a function of distance from reactor

R (cm)	$4\pi R^2 D_\gamma$(r cm²/fission)		
	$\vartheta = 90°$	$\vartheta = 30°$	$\vartheta = 14.5°$
300	2.31×10^{-10}	1.21×10^{-10}	0.795×10^{-10}
400	2.21×10^{-10}	1.19×10^{-10}	0.743×10^{-10}
500	2.16×10^{-10}	1.19×10^{-10}	0.715×10^{-10}
600	2.12×10^{-10}	1.18×10^{-10}	0.697×10^{-10}

different viewing angles, ϑ, and for the prompt fission γ-source distribution.

A.2. *Estimate of fission product γ-contribution to the total dose*

The rate of energy release as photons by fission products may be taken to be the following function of time:[26]

$$E(e) = \frac{0.62}{1 + t} \text{ MeV/sec fission}$$

where t is in seconds and $t \leq 1000$ sec. For comparison, the total photon energy released in prompt fission was taken to be 7.2 MeV.[26]

First, R_s, the ratio of photon energy released per unit time by fission products to the prompt fission rate at the end of approximately 15 min of steady operation is given by

$$R_s = \frac{1}{7.2 \text{ MeV}} \times 0.62$$

$$\int_0^{900} \frac{dt}{1 + t} \text{ MeV} \simeq \frac{0.62}{7.2} \ln 900 = 0.586$$

1005296

and this ratio should apply at the time measurements of the γ-dose rate were made during the experiment.

Next, R_a, the ratio of total photon energy released by fission products in a time T, during which the reactor is critical on a 10-sec doubling time,* to the prompt fission γ-energy released may be shown to be

$$R_a = \frac{1}{7.2 \text{ MeV}} \times \frac{0.62}{t_0(1 - e^{-T/t_0})} \int_0^T e^{-T/t_0} \ln (1 + t - \tau)\, d\tau$$

where $t_0 = 10$ sec/0.693. For an operating time T of 4 min,[27] the above expression is closely equal to

$$R_a = \frac{0.62}{7.2} e^{1/T_0} E_1(1/t_0)$$

Numerical evaluation of these quantities, using values from the data of RITCHIE *et al.*[16] gave the more accurate values of $R_s = 0.632$ and $R_a = 0.219$.

The procedure used in estimating the dose from fission product γ-rays was to assume that the dose attenuation kernel appropriate to this photon distribution is the same as that appropriate to the prompt fission γ-distribution. This should be a good approximation for our purposes.[27] Using this assumption, the leakage calculation for prompt fission γ-rays had only to be scaled by the factors R_s and R_a displayed above in order to obtain the quantities sought.

APPENDIX B

Studies of Na^{24} *Activation in Man-shaped Phantoms*

B.1. *The Los Alamos burro experiment*

An experiment[28] was performed at the Godiva II reactor of Los Alamos Scientific Laboratory to determine whether a phantom composed of a thin shell filled with an aqueous sodium solution could be substituted for a live animal in studies of the relationship between neutron dose and Na^{24} production in the irradiated substance.

A live burro was placed in an aluminum tank which was then filled with NaCl solution and irradiated at 3 m, center to center, from Godiva. Samples of the burro blood serum and of the NaCl solution were prepared and the Na^{24} activities were determined. The burro was removed, the tank refilled with NaCl solution and an exposure made again at the same position. The NaCl solution was sampled and its Na^{24} activity determined. During the second exposure the region in the tank which had previously been filled by the burro was filled by a homogeneous aqueous NaCl solution. The region was, of course, of the same size and shape when filled with NaCl solution as when filled with the burro. If the amount of Na^{24} produced (in the burro and the surrounding NaCl solution) by the first irradiation was, within experimental error, the same as that produced by the second irradiation (when only NaCl solution was present), then the production of Na^{24} in a homogeneous phantom could be considered to be sufficiently quantitatively similar to the production of Na^{24} from the Na^{23} heterogeneously distributed in a live animal that phantoms could be substituted for animals. Concentrations of Na^{24} in the burro and the NaCl solution around it were weighted by the respective volumes and averaged, then compared to the Na^{24} concentration in the full tank of NaCl solution, normalized to the same exposure dose. Relative difference in the amount of Na^{24} produced by the two exposures was 2.9 per cent which is well within the probable experimental error; hence it was concluded that when a man-shaped phantom is filled with a sodium chloride solution, a good approximation to a man is obtained relative to sodium activation.

B.2. *Distribution of* Na^{24} *in phantoms irradiated at Vinča*

Na^{24} concentrations in the phantoms are listed in Tables 9 and 10. All concentrations are corrected to zero time (effective exposure time) and are expressed in μc Na^{24}/mg Na^{23} per rad. Two tables are given because the two

* Private communication with H. D. BROWN and D. NEWBY.

1005291

Table 9. Na^{24} *concentrations in molded phantoms*

Segment	Na^{24} Concentration (μc Na^{24}/mg Na^{23}/rad) $\times 10^5$					
	Calvin I	Remab I	Tyrone I	Calvin II	Remab II	Tyrone II
Head and upper torso	1.44	1.44	1.30	1.55	1.38	1.45
Upper left arm	1.16	1.72	1.75	1.54	1.65	1.82
Upper right arm	1.60	1.28	1.13	1.94	1.45	1.68
Lower left arm	1.18	1.57	1.70	1.78	1.77	1.91
Lower right arm	1.54	1.21	1.17	1.89	1.36	1.84
Lower torso	0.848	0.929	0.781	1.10	0.875	1.01
Gonads	0.842	1.04	1.02	2.08	1.85	1.07
Upper left leg	0.914	1.12	1.16	1.34	1.22	1.23
Upper right leg	1.12	1.03	0.879	1.35	1.27	1.26
Lower left leg	1.13	1.40	1.46	1.60	1.39	1.69
Lower right leg	1.34	1.46	1.18	1.68	1.38	1.63
Average	1.09	1.17	1.09	1.38	1.24	1.28

types of phantoms are segmented slightly differently; in both tables the numerals I and II after the name of the phantom indicate first and second high-power exposures, respectively. The molded plastic phantoms, in Table 9, were designated "Calvin", "Remab" and "Tyrone"; the polyethylene bottle phantom, in Table 10, was called "Bomab". The segments labeled "average" were averaged by mixing and sampling the total solution of each phantom.

APPENDIX C

Intercomparison of French and American Na^{24} *Calibration*

C.1. *Summary of the Saclay* Na^{24} *counting method*

The total amount of Na^{24} present in the bodies of the exposed persons was determined by the French group using a scintillation counter. The detector, a 1.5-in. × 1-in. sodium iodide crystal, was placed at the center of an arc of 1m radius. The individual to be measured lay on the floor facing the detector and curved so as to fit just inside the arc. A twenty-five-channel analyzer was used in conjunction with this detector. As used, the response peak from Cs^{137} γ-rays was in the ninth channel and that from K^{40} γ-rays was in the twentieth channel. The activity measured in the six persons was known to be Na^{24} from energy and half-life considerations. The equipment was calibrated with a polyethylene bottle containing Na^{24} solution of known activity. This bottle was moved along the inside of the arc to measure the angular dependence of the response of the detector. The size of the bottle (15 cm diameter, 25 cm height) was chosen such that the ratio of counts in channels 1–5 to the counts in channels 16–18 was approximately the same whether the activity in the bottle or the activity in the persons was being measured.

Table 10. Na^{24} *concentrations in bottle phantoms*

Segment	Na^{24} Concentration (μc Na^{24}/mg Na^{23} per rad) $\times 10^5$	
	Bomab I	Bomab II
Head	1.40	1.34
Neck	1.33	1.29
Left arm	1.11	1.46
Right arm	1.62	1.58
Upper torso	0.853	1.00
Lower torso	0.755	0.865
Upper left leg	0.846	1.06
Upper right leg	1.11	1.11
Lower left leg	1.03	1.16
Lower right leg	1.25	2.40
Average	0.991	1.10

1005298

C.2. *Studies of the Saclay* Na^{24} *counting geometry*

In order to confirm the method of calibration of the equipment used to measure the Na^{24} activity of the exposed individuals, an experiment was performed at ORNL using a similar crystal, 1.5-in. × 1-in. sodium iodide. A molded plastic phantom (Remab) and the bottle phantom (Bomab) were filled with a homogeneous aqueous solution of Na^{24} of known concentration. The Na^{24} γ-ray activity of the phantoms was measured using the same geometry as had been used to measure the Na^{24} activity of the exposed persons, i.e. the crystal was at the center of an arc of 1 m radius, and the phantom was positioned inside the arc, lying on its side on the floor.

Table 11. *Relative counting efficiency for* Na^{24} *in a bottle and in phantoms*

Energy (MeV)	Relative counting efficiency		
	Bottle	Remab	Bomab
0.366	1.00	0.984	0.997
0.66	1.00	0.969	0.971
1.16	1.00	0.980	1.00
0.366/1.16	2.66	2.66	2.64

The counting efficiency of this geometry was compared to the counting efficiency determined by placing a polyethylene bottle, 15 cm in diameter and 25 cm in height, filled with Na^{24} solution at various positions inside the 1-m arc. The response of the crystal was found to be independent of the position of the bottle along the arc. Integral measurements were made at energies of 0.366, 0.66 and 1.16 MeV. The ratio of the count rate at 0.366 MeV to the count rate at 1.16 MeV was found to be the same for the two phantoms and for the bottle. The results of this experiment, normalized to the counting efficiency for Na^{24} in the bottle, are given in Table 11.

C.3. *Direct intercomparison of Saclay and Oak Ridge* Na^{24} *counting methods*

In order to compare the calibration of the French equipment used to measure the Na^{24} in the bodies of the exposed individuals to the calibration of the ORNL equipment used to determine the Na^{24} concentration in the phantoms, average samples of Calvin II, Remab II and Tyrone II solutions were prepared and sent to Paris for Na^{24} measurements. The results of the French analysis were communicated to us by H. JAMMET and L. JEANMAIRE on 31 May, 1960. An additional solution sample which had been prepared by dissolving irradiated solid NaCl was included in order to obtain a higher disintegration rate. Activity concentrations of the solutions are listed in Table 12.

APPENDIX D

Study of the Neutron Flux Distribution in the Vinča Reactor Room

In order to document neutron data previously given, some of the data from the two high-power runs at Vinča are shown in Figs. 9 through 16. The data presented are from the secondary stations consisting of sulfur, gold and cadmium-shielded gold. Locations of the various stations are shown in Fig. 2.

Table 12. *Cross calibration of French and ORNL equipment for measuring* Na^{24} *concentration*

Solution	ORNL value (μc/ml) × 10^3	French value (μc/ml) × 10^3	ORNL value / French value
Calvin II	1.06	1.03	1.03
Remab II	1.19	1.16	1.03
Tyrone II	1.09	1.05	1.04
Solution from solid NaCl	33.2	33.9	0.98

1005299

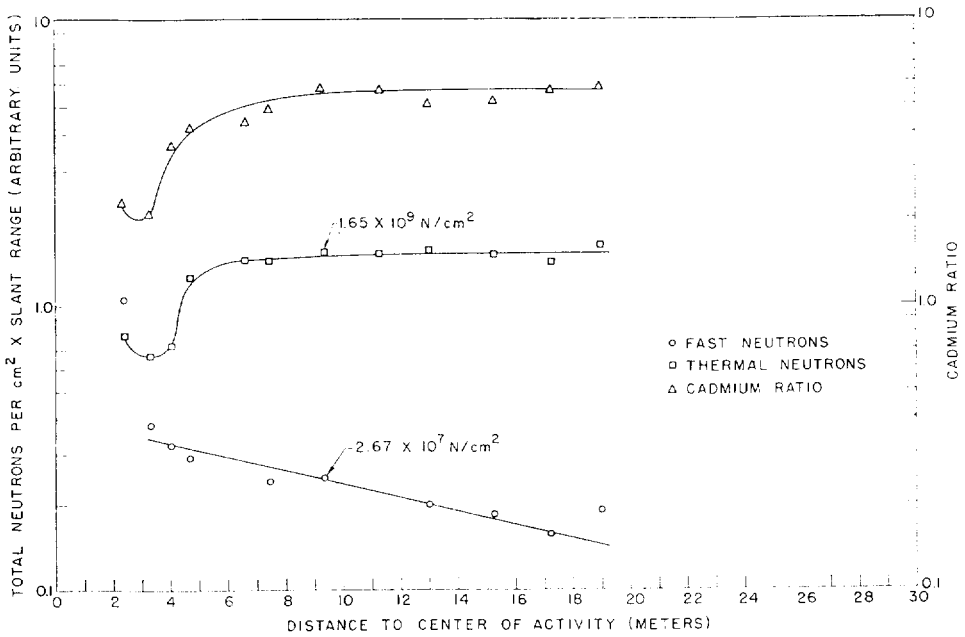

FIG. 9. High-power run no. 1: line running east through LPS-5, 108 cm from floor.

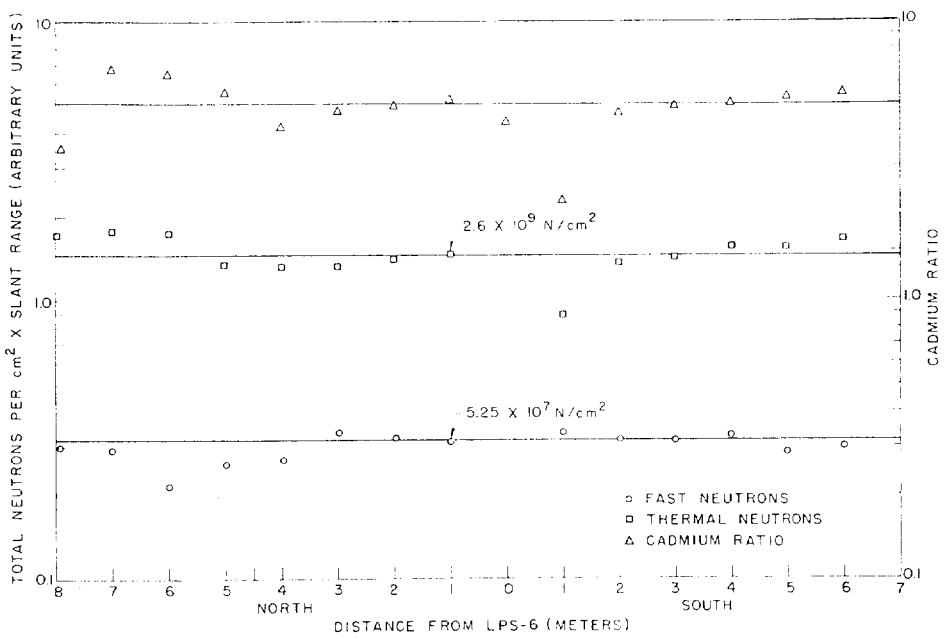

FIG. 10. High-power run no. 1: horizontal traverse 108 cm from floor running north and south through LPS-6.

1005300

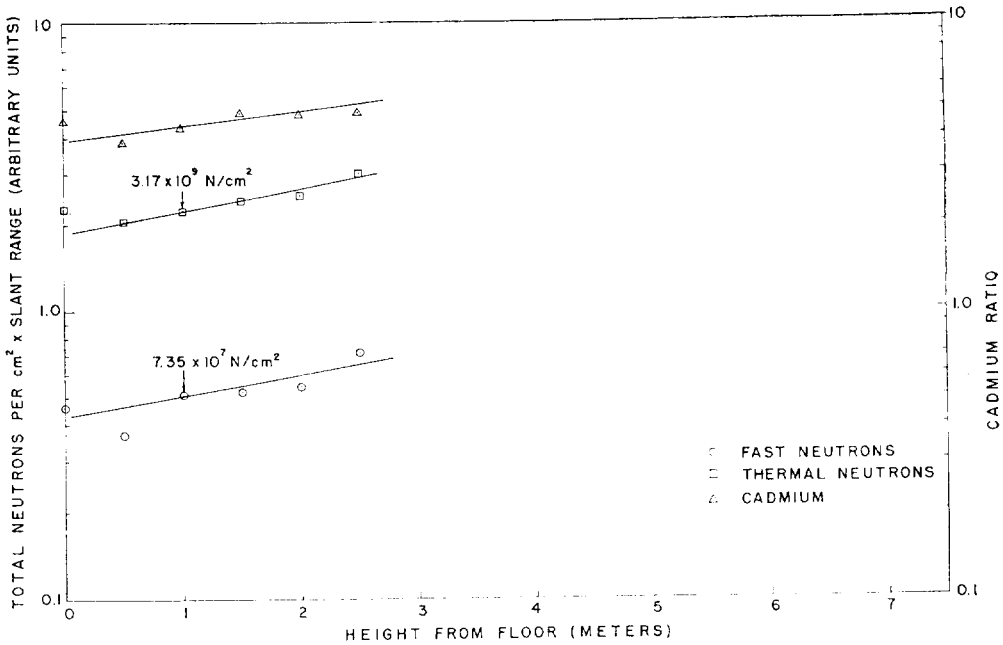

FIG. 11. High-power run no. 1: vertical traverse at LPS-2.

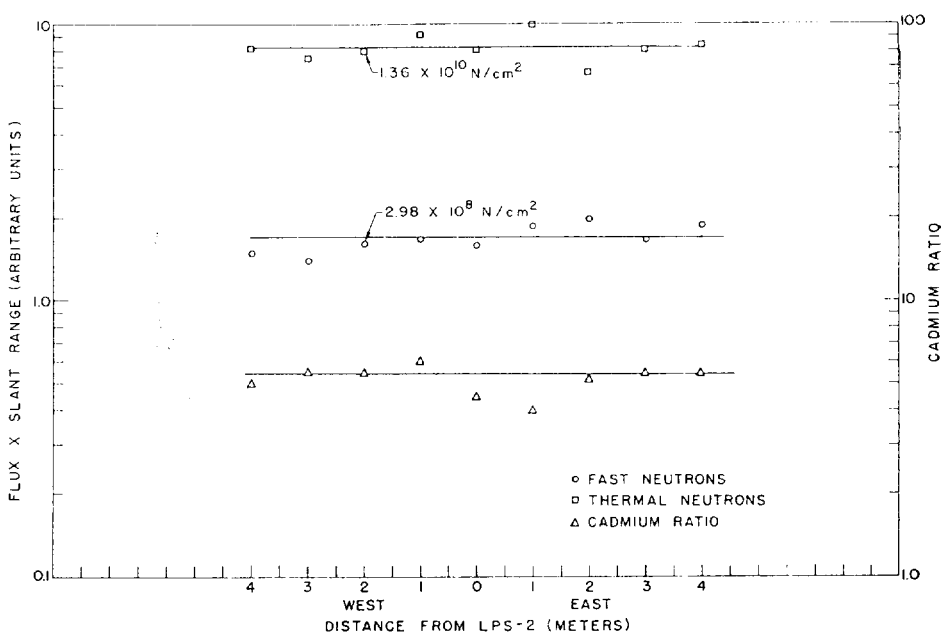

FIG. 12. High-power run no. 2: horizontal traverse 108 cm from floor running east and west through LPS-2.

1005301

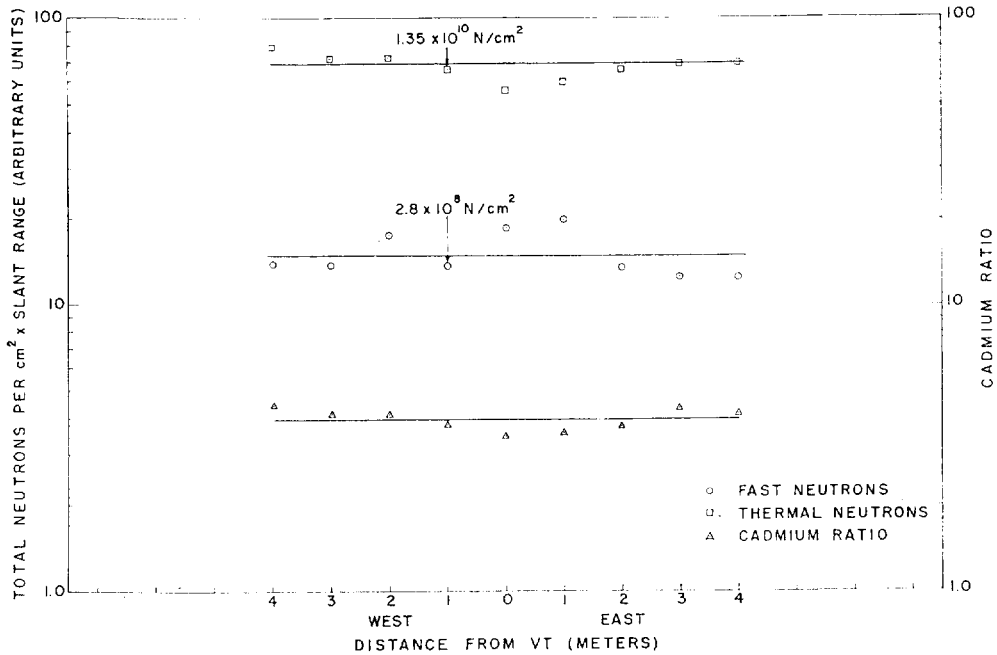

FIG. 13. High-power run no. 2: horizontal traverse 108 cm from floor running east and west through VT.

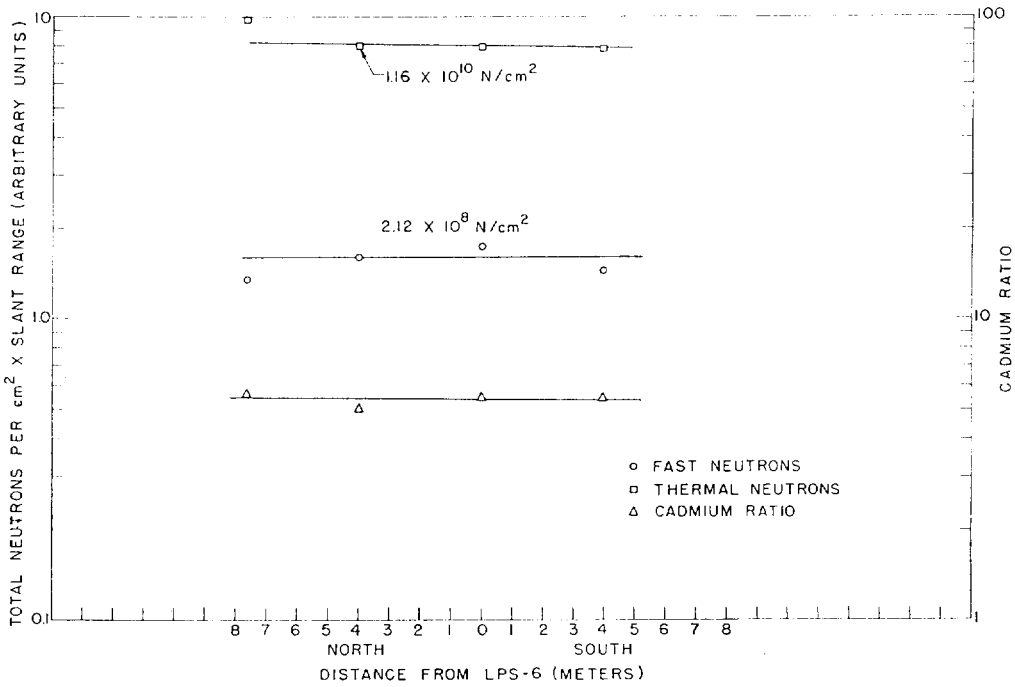

FIG. 14. High-power run no. 2: horizontal traverse 108 cm from floor running north and south through LPS-6.

1005302

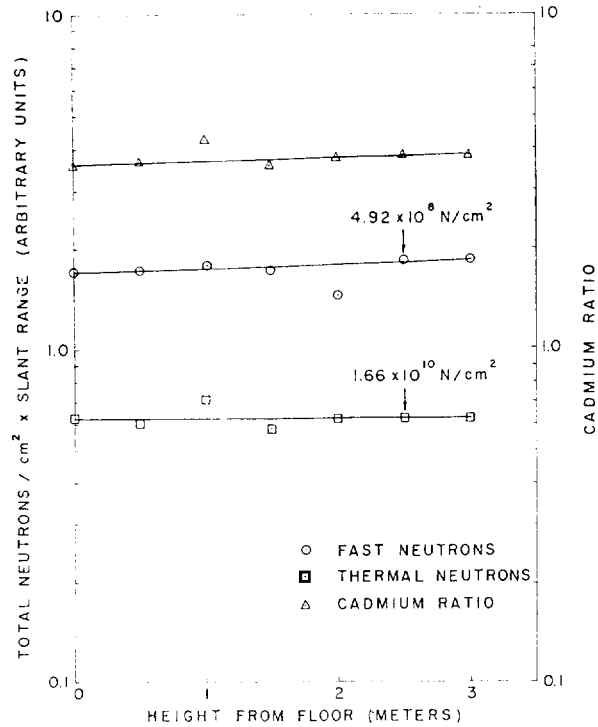

FIG. 15. High-power run no. 2: vertical traverse through VT.

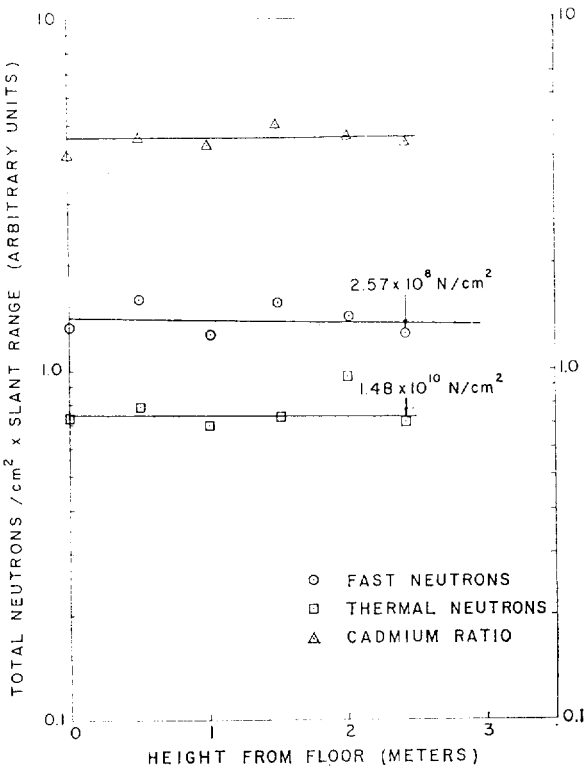

FIG. 16. High-power run no. 2: vertical traverse 3 m west of VT.

1005303

APPENDIX E*

Neutron Measurements with a Tissue-equivalent Phantom

Abstract—Measurements were made through a phantom with fast and slow neutron detectors. These measurements are the basis of a method of dose determination at present in its experimental stages. The Vinča results are therefore presented only to indicate the relative contribution from back-scattered neutrons.

E.1. *Apparatus*

The phantom used was a $\frac{1}{4}$-in. thick Polythene container, 60 cm high of elliptical cross-section, with a major axis 36 cm and minor axis 20 cm. This was filled with an approximately tissue-equivalent liquid (6.24×10^{22} atoms/cm^3 H, 0.669×10^{22} atoms/cm^3 C, 0.169×10^{22} atoms/cm^3 N, 3.25×10^{22} atoms/cm^3 O).

A light but rigid internal framework of Perspex supported a series of small detectors through the phantom, on a line at 15° to the normal in both horizontal and vertical directions to minimize the shielding effect of one detector on another.

The detectors used in the first high level run at Vinča, to measure flux above 0.5 MeV, were 0.5-cm wide track plates wrapped in cadmium foil. Each track plate was a sandwich of two Ilford E1 50-μ emulsions, with glass backing, separated by a 250-μ Polythene radiator, and was oriented at an angle of 45° to the front surface of the phantom. Under these conditions the response is constant with neutron energy between 0.5 MeV and 8 MeV at 1.26×10^{-3} tracks/neutron to within $\pm$ 15 per cent.

The detectors used in the second high level run were gold foils (260 mg/cm^2 thick) to determine the slow neutron distribution. Previous experiments using 0.13 MeV, 2.5 MeV, 14 MeV and Po–Be neutrons have shown that the shape of the curve through a phantom obtained from these gold foils is the same as that given by either manganese foils or sodium samples, despite the difference in resonance integrals.

E.2. *Method*

From the relaxation length of the neutron flux in the phantom, as measured by the track

Table 13. Relaxation length for various neutron energies

Neutron energy	Relaxation length (cm)
1 MeV (monoenergetic)	4.6
2.5 MeV (monoenergetic)	6.3
Po–Be spectrum (mean 4.5 MeV)	10.0
14 MeV (monoenergetic)	20.0

* This Appendix was written by J. W. Smith, United Kingdom Atomic Energy Authority, Harwell, Berks.

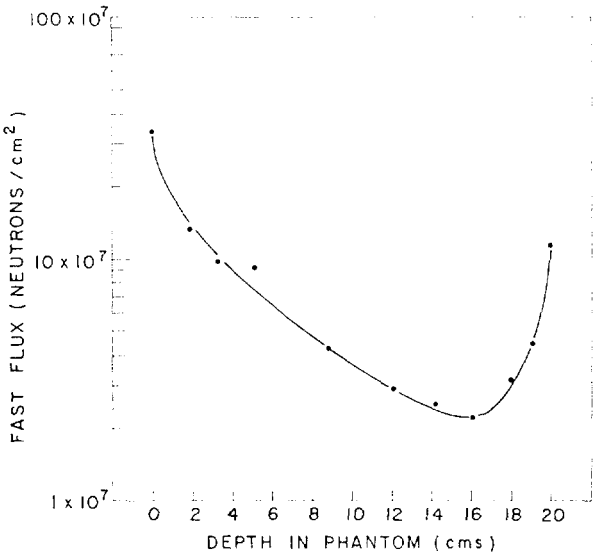

Fig. 17. Flux above 0.5 MeV given by track plates.

1005304

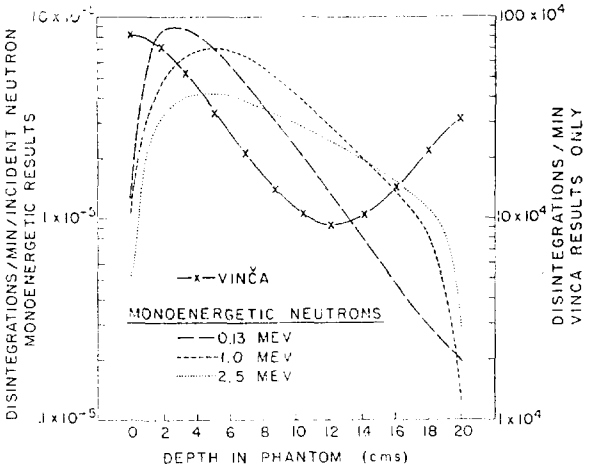

FIG. 18. Distribution of gold foil activity in phantom.

plates, the mean energy of the neutrons with energies greater than 0.5 MeV may be found by comparison with the relaxation lengths obtained by irradiating the phantom with monoenergetic neutrons. The results of these experiments are given in Table 13.

E.3. *Results*

Track plate results from the Vinča experiment are shown in Fig. 17. It can be seen that the back-scattered fast flux is about one-third of the incident fast flux and that the energy indicated by the shape of the curve is considerably lower than the energy of the direct neutrons. It seems possible that the high back-scatter is due to the angle of irradiation; the midline of the phantom was 112 cm above the floor of the reactor hall on the lip of the reactor well so that the angle of elevation to the center of the reactor was about 30°.

Fig. 18 compares the gold foil results from Vinča with previous gold foil curves for neutrons of known energy, all taken with the 20-cm phantom.

Acknowledgments—The authors are pleased to acknowledge the expert services and help given by R. BARKER, G. JENSSEN, G. W. C. TAIT and D. BROWN of the International Atomic Energy Agency in Vienna in making all arrangements for co-operation of the various groups in the experimental investigations; JACKY WEILL, J. FURET, and their associates, the electronics controls group from Centre D'Etudes Nucleaires, Saclay, France, who designed the control equipment and operated the reactor; the Yugoslav Federal Nuclear Energy Commission, expecially S. NAKICENOVIĆ and D. BAUM; V. BABIĆ, Director of the Boris Kidrič Institute, and his scientific staff, particularly D. POPOVIĆ, P. ANASTASIJEVIĆ, and their associates for their full co-operation during the investigation.

We are particularly indebted to H. JAMMET and L. JEANMAIRE, Centre D'Etudes Nucleaires, Saclay, for providing us with Na^{24} data and other information to which the final data are normalized.

Thanks are also due to V. E. ANDERSON of the Oak Ridge Gaseous Diffusion Plant, and H. B. ELDRIDGE, Oak Ridge National Laboratory, for their expert work in performing numerical computations, and to F. J. DAVIS, ORNL, for his advice and assistance in connection with the experimental program.

The authors are most grateful for many valuable suggestions from J. W. SMITH, author of Appendix E, and J. A. DENNIS, United Kingdom Atomic Energy Research Establishment, Harwell, England.

REFERENCES

1. P. P. SAVIĆ, *Bull. Inst. Nucl. Sci. Boris Kidrich* **9,** No. 167 (1959).
2. D. POPOVIĆ, S. TAKAČ, H. MARKOVIĆ, N. RAIŠIĆ, Z. ZDRAVKOVIĆ and LJ. RADANOVIĆ, *Bull. Inst. Nucl. Sci. Boris Kidrich* **9,** No. 168 (1959).
3. H. JAMMET, G. MATHÉ, B. PENDIC, J. F. DUPLAN, B. MAUPIN, R. LATARJET, D. KALIC, L. SCHWARZENBERG, Z. DJUKIC and J. VIGNE, *Rev. Franc. Études Clin. et Biol.* **4,** 210 (1959).
4. G. MATHÉ, H. JAMMET, B. PENDIC, L. SCHWARZENBERG, J. F. DUPLAN, B. MAUPIN, R. LATARJET, M. J. LARRIEU, D. KALIC and Z. DJUKIC, *Rev. Franc. Études Clin. et Biol.* **4,** 226 (1959).

1005305

5. *Accidental Radiation Excursion at the Y-12 Plant* Y-1234 (1958).
6. G. S. Hurst, R. H. Ritchie and L. C. Emerson, *Health Phys.* **2,** 121 (1959).
7. E. B. Wagner and G. S. Hurst, *Rev. Sci. Instrum.* **29,** 153 (1958).
8. E. B. Wagner and G. S. Hurst, *Health Phys.* In press.
9. L. H. Ballweg and J. L. Meem, *A Standard Gamma-Ray Ionization Chamber for Shielding Measurements.* ORNL-1028 (1951).
10. G. S. Hurst, J. A. Harter, P. N. Hensley, W. A. Mills, M. Slater and P. W. Reinhardt, *Rev. Sci. Instrum.* **27,** 153 (1956).
11. P. W. Reinhardt and F. J. Davis, *Health Phys.* **1,** 169 (1958).
12. G. S. Hurst and R. H. Ritchie (Editors), *Radiation Accidents: Dosimetric Aspects of Neutron and Gamma-Ray Exposures.* ORNL-2748 (1959).
13. C. L. Daws, J. M. Bookston and R. E. Smith, *GNU-II, A Multigroup One-Dimension Diffusion Equation.* GMR-101 (1957).
14. A. M. Weinberg and E. P. Wigner, *The physical Theory of Neutron Chain Reactors.* The University of Chicago Press, Chicago, Illinois (1958).
15. H. D. Brown and D. Newby, International Atomic Energy Agency, Vienna, Austria. Private communication.
16. R. H. Ritchie, H. B. Eldridge and V. E. Anderson, Calculation of the radiation yield from fission assemblies and comparison with experiments. *Proceedings of the International Symposium on Selected Topics in Radiation Dosimetry, Vienna, Austria, June,* 1960. To be published.
17. G. S. Hurst, *Brit. J. Radiol.* **27,** 353 (1954).
18. E. B. Wagner and G. S. Hurst, *Health Phys.* **2,** 57 (1959).
19. D. Popović, Boris Kidrić Institute, Vinča, Yugoslavia. Private communication.
20. F. C. Maienschein, R. W. Peelle, W. Zobel and T. A. Love, *Second United Nations International Conference on Peaceful Uses of Atomic Energy* Vol. 15, pp 366–372. United Nations, New York (1958).
21. G. A. Bartholomew and L. A. Higgs, *Compilation of Thermal Neutron Capture Gamma Rays.* CRGP-784 (1958).
22. G. W. Grodstein, *X-Ray Attenuation Coefficients from* 10 keV *to* 100 MeV. National Bureau of Standards Circular 583, Washington, D.C. (1957).
23. National Bureau of Standards Handbook 63, *Protection Against Neutron Radiation up to* 30 *Million Electron Volts.* Washington, D.C. (1957).
24. H. Goldstein and J. E. Wilkins, Jr., *Calculations of the Penetration of Gamma Rays.* NYO-3075 (1954).
25. H. Goldstein and J. E. Wilkins, Jr., *Calculations of the Penetration of Gamma Rays* p. 64. NYO-3075 (1954).
26. H. Goldstein, *Fundamental Aspects of Reactor Shielding* p. 63. Addison-Wesley, Cambridge, Massachusetts (1959).
27. H. Goldstein, *Fundamental Aspects of Reactor Shielding* p. 58 *et seq.* Addison-Wesley, Cambridge, Massachusetts (1959).
28. F. W. Sanders and J. A. Auxier, Neutron activation of sodium in anthropomorphous phantoms. *Health Phys.* To be published.

1005306